A HIGHER FIDELITY APPROACH FOR INCORPORATING TIP SHROUD GEOMETRY INTO AERODYNAMIC FLUTTER COMPUTATIONS OF ROTATING TURBOMACHINERY

A. Rozendaal - A. Torkaman* - G. Vogel* - A. Lo Balbo***

*Power Systems Mfg., LLC, Ansaldo Energia Group, Jupiter, FL, USA
**Ansaldo Energia, Genoa, Italy

ABSTRACT

Computational Fluid Dynamics (CFD) solvers can be used for predicting aerodynamic stability of rotating turbomachinery. Frequency-domain methods offer increased computational efficiency for flutter applications. They enable the unsteady aerodynamic response for an entire un-shrouded blade row to be computed using only a single sector numerical passage. The relative motion of the blade is simulated through a mesh-morphing procedure according to the blade's structural mode shape. However surface conformity along the periodic planes of the passage is required. Such a requirement is especially difficult to satisfy for blades with interlocked tip shrouds that suppresses the periodicity during the morphing cycle. For this reason, such flutter simulations are often performed without a blade tip shroud. This paper examines the effects of the neglected tip shroud assumption on the aerodynamic flutter characteristics of a shrouded turbine blade by implementing a method in which to incorporate the interlocked tip shroud into the CFD simulation.

KEYWORDS

Aerodynamic flutter, Shrouded Turbine Airfoil, Harmonic Balance

NOMENCLATURE

CFD	Computational Fluid Dynamics
FEA	Finite Element Analysis
HB	Harmonic Balance
IGT	Industrial Gas Turbine
LSB	Last Stage Blade

INTRODUCTION

Flutter is a major issue in the design and optimization of last stage turbine blades (LSB) due to the transonic fluid velocities and low natural frequencies that are characteristic of tall and slender blades. Flutter is an aeroelastic phenomenon that results from the interaction between inertia, stiffness and aerodynamic forces that act on the blade as described by Collar (1946). Historic research into understanding and computing the underlying unsteady pressure distributions that contribute to these aeroelastic effects has been summarized by Marshall and Imregun (1996).

Unsteady pressure distributions on the airfoil surface are generally determined to be a primary influencing factor on the aerodynamic work interaction between the fluid and the blade. Energy-based methods such as from Carta (1967) are typically employed for such calculations. Accurate predictions of the phase and magnitude of the unsteady pressure fields are therefore necessary conditions for high fidelity flutter calculations. Time-linearized Euler methods from Marshall and Giles (1998) and Ning and He (1998) and Navier-Stokes based methods have been successful in capturing the unsteady pressure fields surrounding an oscillating airfoil. Although time-linearized

Euler methods have been popular due to their increased computational efficiency, 3D Navier-Stokes solvers are generally preferred on account of their higher accuracy in predicting unsteady pressure as shown by McBean et al. (2005). Frequency domain solvers based on harmonic balance methods have since been developed to preserve the accuracy of time-marching Navier-Stokes solvers, but at a fraction of the computational cost as reported by Hall et al. (2002). This method assumes flow periodicity as described by a set of Fourier coefficients of the associated harmonics in the frequency domain.

Regardless of the numerical method applied, a single sector passage is commonly used to represent the entire cascade in the analysis. However, certain modelling limitations often prevent higher-fidelity features such as tip shrouds from being included in the simulation. Since tip clearance flow is known to influence aerodynamic damping predictions (Teixeira and Kielb, 2017), neglecting tip shrouds from the analysis undoubtedly introduces a source of error in the flutter solution.

To understand the reason for tip influence, it is noted that in addition to 2D distributions of unsteady pressure around the airfoil, span-wise distributions on a three dimensional airfoil also have a significant effect on flutter response. Research by Gnesin et al. (2000) shows that the most critical portion of a blade with unstable work interaction is typically in the 70-100% span of the airfoil. This is the same region where the pressure distribution is mostly influenced by the over-tip flow.

In addition to temporal distributions of unsteady pressure over the full cycle of vibration, aerodynamic damping has also been determined to be influenced by steady-state sources. Specifically, stage pressure ratios and resulting steady pressure distributions play an important role in influencing relative exit Mach numbers and passage shock wave interactions (Waite and Kielb, 2015). In the case of shrouded LSB's, the presence of the tip shroud significantly alters the flow field around the airfoil tip thereby influencing the steady and unsteady pressure distributions around the airfoil. This is especially true in the higher span regions of the blade (70-100%) which play a critical role in overall flutter stability. Accurate modeling of the tip region with the complete shroud geometry is therefore critical in acquiring higher fidelity predictions for the aerodynamic work interaction and overall flutter response.

CURRENT SIMULATION LIMITATIONS

Periodic Plane Approach

Multistage turbomachinery flow in computational space is commonly simulated by representing all blade rows of the machine as single sector passages. This approach is generally valid for steady-state analyses as it follows the assumption that all blades around the wheel remain identical in shape, are subject to identical flow physics, and remain stationary in the relative frame of reference. The application of periodic boundary conditions provides axisymmetric closure for each flow field in order to facilitate a reasonable estimate of the flow around the entire circumference of the machine, but at a fraction of the computational cost. An example of this type of treatment is illustrated by the aft-stage industrial gas turbine model shown in Figure 1.

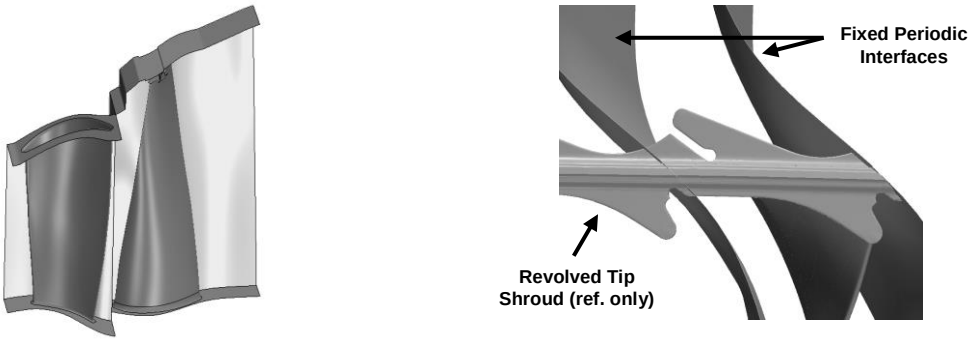

Figure 1: Example vane and blade modelled as single passages with periodic planes (left), and tip shroud interaction with periodic planes (right).

The implementation of periodic boundary conditions on either side of the blade passage enables the flow solution to map directly from one face to the other through the corresponding rotation angle. This implies that the periodic interfaces may intersect the tip shroud at an arbitrary location provided that conformity between the two periodic surfaces is preserved. Such geometrical periodicity can be verified by inspecting the continuation of the surface geometry as demonstrated by the revolved tip shroud in Figure 1. Initially-established periodic surfaces of a steady-state simulation will therefore remain conformal given that all boundaries, by definition, remain fixed. However, when transient behavior is introduced in the form of blade vibratory motion for example, it becomes difficult to maintain conformity between the fixed periodic surfaces. Special treatment of the tip shroud is therefore required in order to compensate for the blade movement if the higher aerodynamic fidelity (on account of the fluid-tip shroud interaction) is to be maintained. One such measure is presented in this paper.

Relative Blade Motion

The blade's relative vibratory motion is considered at more detailed levels of analyses such as when flutter characteristics are being investigated. In such cases, the aerodynamic response to a blade's relative motion (as described by its mode shape and vibration frequency) is analyzed to determine whether or not the movement is being damped or excited; the latter of which corresponds to the onset of flutter. Some CFD solvers offer the ability to introduce such blade motion through a mesh morphing procedure. STAR-CCM+®, for example, incorporates this feature as part of their Harmonic Balance Flutter model. In this case, the user inputs the real and imaginary displacements of a given structural mode shape, and the program physically morphs the mesh to a specified number of time levels representative of the corresponding periodic motion. The aerodynamic work of the complete periodic cycle is then calculated by a mixed frequency/time domain CFD solver, in which the transient flow-field is represented as a Fourier series in the frequency domain. Additional details regarding the Harmonic Balance approach including theory and validation efforts are provided by Hall et al. (2002), Weiss et al. (2011) and Custer et al. (2012).

One of the key benefits of implementing this type of solver for flutter applications is the ability to simulate travelling pressure perturbations tangentially across an entire blade row using only a single passage computational domain. This differs from a classical time-marching fluid-structure interaction approach for example, where multiple passages would be required to achieve spatial periodicity. The use of phase-lagged boundary conditions may be coupled with some time-marching methods in order to simplify the domain to a single sector passage, however the aforementioned transient tip shroud limitations would be inevitably encountered.

For the Harmonic Balance model, a single sector passage is achieved with the application of time-lagged periodicity conditions defined on the periodic boundaries. In considering $\widehat{\boldsymbol{W}}$ as the set of Fourier coefficients related to a given solution vector of conservative variables, spatial periodicity is applied with the following definition from Weiss et al. (2011):

$$\widehat{\boldsymbol{W}}(r, \theta + G, z) = \widehat{\boldsymbol{W}}(r, \theta, z) e^{\frac{i\sigma}{\omega}} \tag{1}$$

The left and right-hand sides of Eqn. (1) represent the solutions on the lower and upper periodic boundaries in cylindrical space respectively. The remaining variables include the radial, azimuthal, and vertical coordinates, *r*-θ-*z*, blade pitch *G*, interblade phase angle σ, and fundamental frequency ω. With this approach, the solutions at each discrete time level of the mesh morphing cycle become coupled through a phase-shifted Fourier transformation process (Weiss et al., 2011).

Domain Simplification

It can be seen upon closer inspection of Eqn. (1) that the solution across a periodic boundary is retained for a fixed set of *r*-*z* coordinates. This introduces a requirement that both periodic planes must remain conformal (or near conformal) during a blade motion cycle in order for the phase-shift transformation to be effective. Additional geometrical restrictions arise from the fact that the

morphing algorithm only displaces the computational nodes of the initially-defined mesh. Hence any variation of geometrical displacement that may occur through the periodic surfaces, such as the transient incursion of a neighboring tip shroud for example, is not accounted for by the morphing procedure. The simplest way to avoid these limitations comes with the removal of the tip shroud altogether as is demonstrated by Figure 2. In doing so however, all accompanying aerodynamic fidelity resulting from the fluid-tip shroud interaction is consequently lost.

Limitations involving tip shroud modelling are especially common when utilizing fully-structured CFD solvers (as is often the case for most in-house codes). Upon realizing the difficulty involved in retaining complex geometrical details in a structured mesh environment, the tip shroud is often neglected from the aerodynamic simulation under the assumption that a reasonable estimate of a blade's flutter characteristics can be obtained without it. This often causes the corresponding error to be overlooked in order to give way to practicality. The focus of this paper is to present a method in which to mitigate this error.

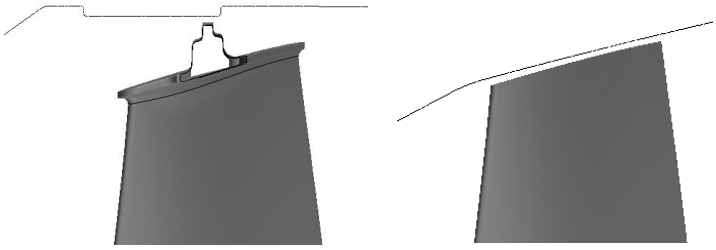

Figure 2: Shrouded blade with pierced periodic boundaries (left), and neglected tip shroud approach (right).

PROPOSED TIP SHROUD TREATMENT

This section introduces a method that allows interlocked tip shroud geometry to be incorporated into flutter simulations while still maintaining conformity along the periodic boundaries.

Mesh Morphing & Mode Shape

The HB Flutter solver couples its mesh morphing capabilities with the Harmonic Balance methodology to compute the pseudo-transient aerodynamic response of a blade's relative motion. The motion itself is defined by the structural mode shape and natural frequency of the system for a given operating condition. This is typically computed using external Finite Element Analysis (FEA) software in which full tip shroud definition with appropriate contact constraints are accounted for. An example of a solved mode shape for a shrouded industrial gas turbine blade, as well as its progression around the wheel, is shown in Figure 3 (left and center respectively).

The mode shape is input into the aerodynamic simulation as a list of control points and their corresponding real and imaginary displacements. Inputting other parameters including the vibration frequency, interblade phase angle, and desired number of intermittent time levels enables the program to conduct the morphing operation. An example of a morphing cycle for an unshrouded blade is shown in Figure 3 (right).

FEA solutions such as the ones seen in Figure 3 are often mass-normalized, and so the resulting displacements sometimes appear to be abnormally large. A scale factor is applied by the user to counter this effect and reduce the deflection amplitude to a range more suitable for numerical analysis. A maximum displacement amplitude between 1-3% tip chord has proven to be sufficient in capturing detailed pressure perturbations from the resulting motion, but also small enough to preserve cell quality during the mesh morphing procedure. The effect of the scaling factor on the aerodynamic solution is later adjusted for when calculating the normalized damping coefficient of the blade.

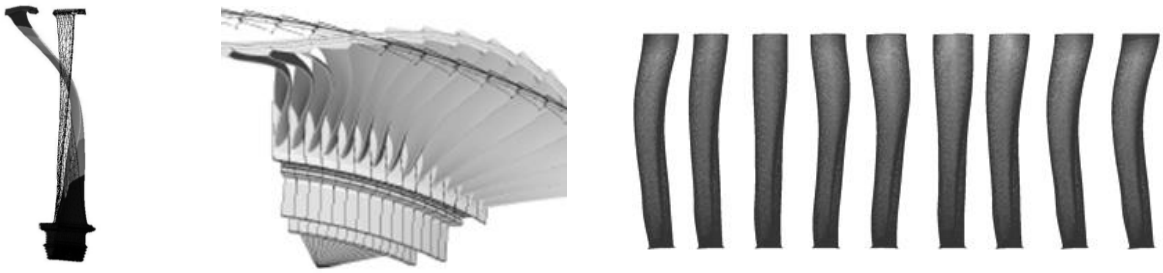

Figure 3: Example mode shape of a shrouded turbine blade (left), progression of a mode shape around the wheel (center) and morphing cycle with nine time levels (right).

Surface Motion Specification

The HB flutter application provides a list of options to control how morphing is performed on a given boundary. For example, controlled motion is specified using a *Displacement* option, in which the grid vertices are physically relocated in accordance with user defined input. This type of treatment is necessary for defining airfoil flutter motion as previously discussed. Alternatively, a *Fixed* condition is applied for boundaries that do not undergo any form of relative motion. Examples include inlet and exit planes, hub and case surfaces, and periodic boundaries. A third *Floating* option is also available in which resulting grid motion is interpolated by the program near fixed and displacing boundaries. A suitable application for this condition may include a root fillet that is bounded by a displacing airfoil and a stationary hub platform as it can mitigate the risk of obtaining poor quality cells during the mesh motion. A more detailed summary of all mesh morphing capabilities is provided by the STAR-CCM+® user guide (Siemens PLM, 2018).

When performing flutter analysis on a blade with an interlocked tip shroud, a combination of all three options is recommended in order to adhere to the periodic boundary constraints described earlier. The proposed tip definition essentially sub-divides the tip shroud region into two surfaces: a thin layer that remains fixed to the periodic plane, and a floating surface that deforms according to the prescribed airfoil motion. An example of this treatment is demonstrated in Figure 4.

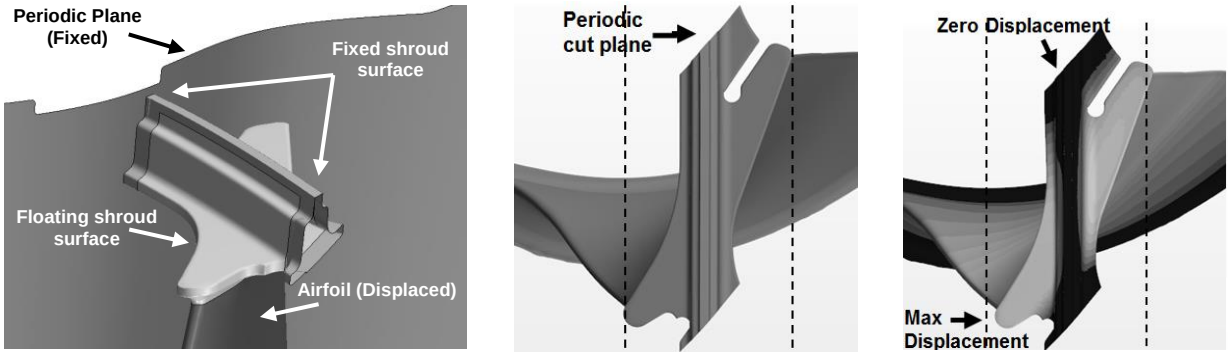

Figure 4: Mesh morphing treatment for a blade with an interlocked tip shroud (left). Before mesh morphing (center), after mesh morphing (right).

The fixed region definition shown in Figure 4 (Left) includes a thin layer of the shroud surface in contact with the periodic boundaries, as well as the upper-most surface of the knife edge. This region is typically prone to a high aerodynamic gradient due to the small gap that exists between the knife edge and the outer case. The application of a fixed constraint assists in preserving the mesh quality intended to capture this gradient before morphing is performed. The movement of the floating surface is therefore interpolated between this area and the displacing airfoil vertices.

Given that the scaled deflections of the tip shroud are generally quite small (usually on the order of 1-3 mm), the overall motion of the tip shroud does in fact remain reasonably consistent with the true tip motion as prescribed by the solved FEA mode shape. Typical displacement levels

experienced by the tip shroud are shown in Figures 4 (Center & Right). Thus even with the application of the fixed surface constraint, the proposed method effectively establishes a means of obtaining a higher-fidelity representation of the aerodynamic flow structure that surrounds the airfoil tip region during the flutter motion. The fluid-tip shroud interaction would otherwise be neglected by the unshrouded approach. Further, the physical mode shape of the airfoil itself is not in any way altered by the proposed morphing treatment as it remains the product of the FEA analysis.

SOLUTION COMPARISON

Work per Cycle Definition

A blade's flutter characteristics are estimated by resolving both the steady and transient pressure fields surrounding the blade, and evaluating their resulting influence on the overall exchange of energy with the working fluid. Although there are a handful of sources that may contribute to the level of unsteadiness, a common factor considered for this type of analysis relates to the interaction of travelling pressure perturbations produced by the blade's relative motion. The transfer of energy resulting from the fluctuating pressure field is measured by computing the corresponding *work per cycle*, which is essentially the dot product of the local force and velocity vectors through one vibration cycle of the blade's motion as defined in Kielb et al. (2006). The general form of this calculation is as follows:

$$W_{cycle} = \int_A \int_0^T -\left(\overrightarrow{\dot{\Phi}} \cdot \vec{N} P\right) dt dA \tag{2}$$

where $\overrightarrow{\dot{\Phi}}$, $\vec{N}$, and P are the velocity (motion displacement derivative), normal vector, and surface pressure respectively. For harmonic motion, these parameters are expanded as:

$$\overrightarrow{\dot{\Phi}} = \frac{1}{2}\left(\vec{\phi} e^{-i\omega t} + \bar{\vec{\phi}} e^{i\omega t}\right) \tag{3}$$

$$\vec{N} = \vec{N}_{steady} + \frac{1}{2}\left(\vec{n} e^{-i\omega t} + \bar{\vec{n}} e^{i\omega t}\right) \tag{4}$$

$$P = P_{steady} + \frac{1}{2}\left(p e^{-i\omega t} + \bar{p} e^{i\omega t}\right) \tag{5}$$

The additional bar over the variable denotes the complex conjugate from Kielb et al. (2006). The substitution of the above expressions into Eqn. (2) verifies an earlier statement that the work per cycle is indeed a function of both the combined steady and unsteady pressure contributions for blades with complex mode shapes (as is often the case for shrouded blades). The effect of these contributions will be discussed later. The HB Flutter solver computes the work per cycle over the surface of the blade as:

$$W_{cycle} = T \sum_f \hat{q}_f^0 \tag{6}$$

where $\hat{q}_f^0$ is the mean of the integrand representing the power at each specified time level, *T*. The power at each time level, $\hat{q}_f^*$, is defined as:

$$\hat{q}_f^* = \hat{p}_f^* \left(\mathbf{v}_f^*\right) \mathbf{a}_f^* \tag{7}$$

where $\hat{p}_f^*$, $\mathbf{v}_f^*$, and $\mathbf{a}_f^*$ are the pressure, relative velocity, and area respectively, of a given face on the surface of the blade (Siemens PLM, 2018). A negative value of work per cycle signifies that energy is transferred from the blade to the fluid over one period of motion. In other words, the blade is said to be aerodynamically stable. A positive value on the other hand corresponds to the aerodynamically unstable case where the blade's internal stiffness may be overcome by the kinetic

energy of the fluid. There exists a small range immediately beyond the point of aerodynamic instability in which the mechanical properties of the blade may be sufficient enough to dampen the imposed aerodynamic behavior. However once this mechanical damping threshold is exceeded, the blade's amplitude of vibration in response to a given frequency excitation may grow to the point of structural failure. This degree of self-excitation is referred to as Flutter.

A typical measure for the rate at which the vibration amplitude may change throughout the motion cycle is obtained with the evaluation of the system's *logarithmic decrement*. This value essentially couples the influence of the blade's aerodynamic and mechanical damping properties into a global dynamic response calculation. A positive value for the logarithmic decrement indicates that the system is damped and the corresponding amplitude of vibration would decrease in response to a given excitation. A negative value would therefore signify an increase in amplitude over time (flutter).

The mechanical damping contribution to the logarithmic decrement is often difficult to calculate, but it is generally known to be very small compared to the aerodynamic contribution. It is for this reason that the aeroelastic stability of a blade is typically assessed only through the evaluation of the aerodynamic damping. A common definition of this parameter for turbomachinery applications includes the following definition from Carta (1967):

$$\delta_{aero} = -\frac{N_{blades}\, W_{cycle}}{4\,\overline{KE}} \tag{8}$$

where, W_{cycle} is the work per cycle previously defined in Eqn. (6), N_{blades} is the total number of blades around the wheel, and $\overline{KE}$ is the average internal kinetic energy of the blade. The work per cycle is of course additionally normalized by the square of the amplification factor applied during the mesh deformation process (if any).

Steady Pressure Comparison

The significance of the steady pressure contribution to the work per cycle calculation is better understood by referring to Eqns. (6) and (7). Specifically, the computed work per cycle is observed to be heavily dependent on the magnitude of the pressure field surrounding the blade, as well as the surface area on which it acts. By this notion, it becomes clear that any change to the blade geometry that may affect the surrounding pressure field, such as the inclusion/exclusion of a tip shroud for example, would directly influence the predicted aeroelastic response. The displacement derivative term $\mathbf{v}_f^*$ is governed by the vibratory motion associated with the blade's structural mode shape, and would remain unaffected if the tip shroud were removed from the aerodynamic simulation.

Two separate examples illustrating the differences in steady surface pressure distributions with and without simulated tip shrouds are shown in Figure 5. The first comparison between Figure 5 (top left and top right) corresponds to the LSB with the scalloped tip shroud previously shown in Figure 4. The second case in Figure 5 (bottom left and bottom right) is provided for additional reference showing an equivalent comparison of a similar turbine blade with a more axisymmetric tip shroud. Both blades maintain a very similar span (~0.5m) and aspect ratio (~4 ref from mid chord). The simulations were performed on a polyhedral grid using a 2nd order realizable k-ε turbulence model ($Y+ < 1.5$). The inlet and exit boundary conditions were corrected to best represent the true design-point operating condition of each blade. The tip gaps for the unshrouded simulations were further adjusted to provide equivalent comparisons of solution variables with the shrouded scenarios.

Both comparisons consistently produced a concentrated area of low pressure near the trailing edge (depicted by the darker shade) resulting from the removal of the tip shroud. This is on account of the accelerated over-tip vortex flow structure that is common to unshrouded blades. A thorough explanation into the effect of the tip gap flow structure on the aerodynamic damping of unshrouded blades is provided by Teixeira and Kielb (2017).

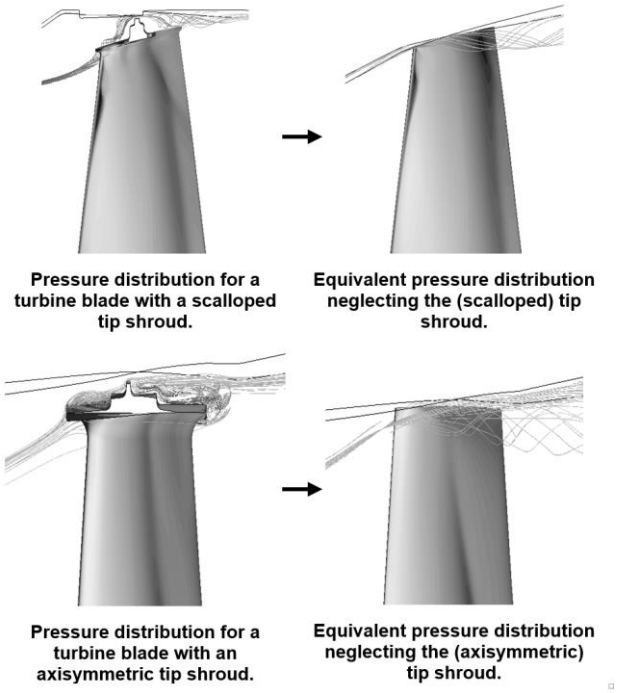

Figure 5: Two examples of shrouded blade modelled with and without their scalloped (top) and axisymmetric (bottom) shrouds.

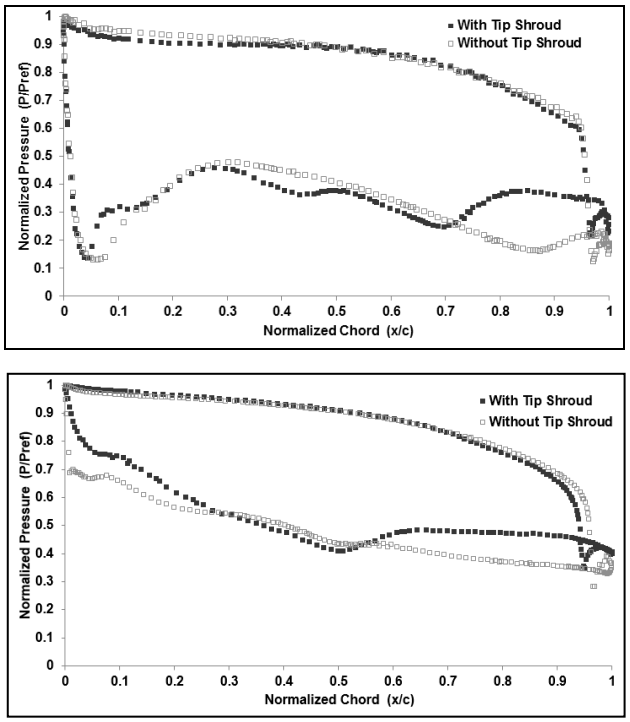

Figure 6: Comparison of normalized static pressure at 95% span for scalloped (top) and axisymmetric (bottom) shrouds.

A chord-wise comparison between the steady-state pressure fields at 95% span for both blades are shown in Figure 6. The differences observed along the suction surface curves of Figure 6 correspond to the interaction of the surface pressure field with the over-tip flow structure that results from the neglected tip shroud assumption. The distributions along the pressure surfaces however remain fairly unaffected with an exception of the region where the over-tip vortex core is seen to form ($x/c \approx 0.0$-0.15). From this comparison it is evident that the removal of the tip shroud from the steady-state analysis has indeed affected the chord-wise pressure ratio distribution near the trailing edge of the tip region, which directly influences the blade's associated loading characteristics and corresponding center of pressure location. The observed differences in pressure distributions begin to diminish below roughly 70-80% span.

Transient Pressure Comparison

The implementation of relative blade motion introduces a fluctuating pressure field that contributes to the work exchanged with the fluid over one vibration period. The magnitude of fluctuation is dependent not only by the mode shape and frequency of the response, but also by the variation of the blade loading that is encountered throughout the motion. Since the base loading was already identified through the steady-state analysis to change as a result of the neglected tip shroud assumption, any inconsistencies in oscillation between the two pressure fields would further contribute to a difference in energy exchanged with the fluid. The magnitude of the first pressure harmonic experienced by the scalloped blade for a given mode shape is shown in Figure 7 (Left). An equivalent comparison for the case without the tip shroud is shown in Figure 7 (Right). Figure 7 clearly demonstrates the influence of the tip shroud flow structure on the fluctuating pressure field near the trailing edge of the blade. The darker regions in the figures represent areas that experience a narrow range of pressure oscillation during the blade motion, while lighter shades signify regions of greater fluctuation. Figure 8 provides an overlapped comparison of the minimum and maximum range of transient pressure distributions experienced throughout the entire motion cycle of each blade at 95% span.

Figure 7: First pressure harmonic magnitude with (Left) and without (Right) the tip shroud modelled.

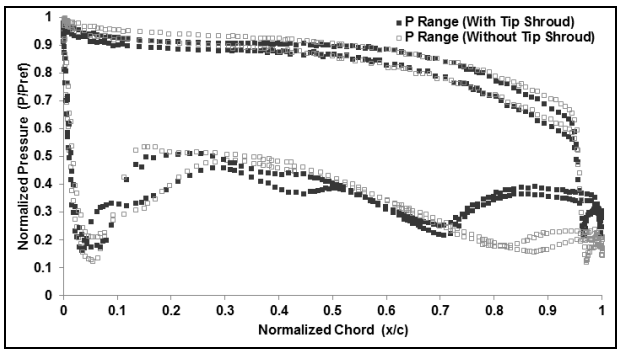

Figure 8: Comparison of min and max pressures experienced during blade motion at 95% span.

The dark points in Figure 8 correspond to the min and max pressure range experienced for the case with the tip shroud (Figure 7 Left) and the light grey points for the case without the tip shroud (Figure 7 Right). Again, it can be seen that the majority of differences in pressure fluctuations occurred along the suction surface of the blade. Specifically, the removal of the tip shroud is seen to have minimized the range of fluctuation around 40% and 70% chord, which corresponds to the region directly in front of and behind the knife edge of the shroud seen in Figure 7 (Left). The trailing edge (near 90% chord), however, experienced a slightly higher range of oscillation as a result of the neglected tip shroud assumption.

Since it was determined that the surface work distribution for a prescribed mode shape is influenced by both the steady and unsteady contributions of the surrounding pressure field (verified by Eqns. 2-5), it is expected that the observed changes in the pressure loading resulting from the inclusion/exclusion of the tip shroud would directly influence the predicted aerodynamic stability of the system. A comparison of the surface work distribution for each case cannot be directly plotted as the program does not yet offer the ability to post-process this quantity, however differences in stability may be equally assessed by comparing the solved aerodynamic damping coefficients defined by Eqn. (8).

Aerodynamic Damping

Global stability of a blade is generally evaluated by computing the work per cycle for a much larger range of mode shapes that may be encountered during engine operation. This typically requires that the aerodynamic analysis be repeated for the complete sweep of nodal diameters corresponding to several structural mode families (e.g. 1st bending, 1st torsion). It is this reason that generally distinguishes flutter analysis as being computationally expensive.

The complete nodal diameter sweep for the 1st torsional mode of another industrial LSB of similar span and aspect ratio is provided in Figure 9. A comparison between the predicted aerodynamic damping was made both with and without a simulated (scalloped) tip shroud. The shrouded analysis was performed using the HB Flutter solver with the proposed shroud treatment discussed earlier. The reference unshrouded analysis was performed with TRAF (Pinelli et al., 2009), an in-house non-linear time domain based Navier-Stokes code using structured mesh. This code does not allow exclusive implementation of tip shroud geometry, so an equivalent tip gap was modeled instead. Additional unshrouded data points were obtained with the HB Flutter solver to verify that any major differences in the predicted damping values were the result of the neglected tip shroud assumption, and not the solver itself. The vertical axis in Figure 9 has been normalized to protect the proprietary of the true solution, however the physical shapes and relative differences remain unaltered to provide a real comparison of the un-optimized aerodynamic damping results.

Figure 9 shows a close comparison in the predicted aerodynamic damping solutions between the shrouded and unshrouded simulations. The solved damping coefficients for the range of normalized

nodal diameters between ±[0.0, 0.3] and ±[0.8, 1.0] exhibited the closest consistency with a maximum relative error of about 8%. A gradual increase in error was observed near the minimum and maximum points of stability, which experienced relative errors ranging between 20-40%.

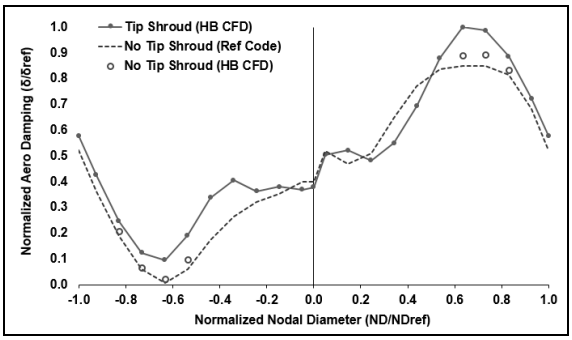

Figure 9: Comparison of shrouded (scalloped) and unshrouded aerodynamic damping predictions.

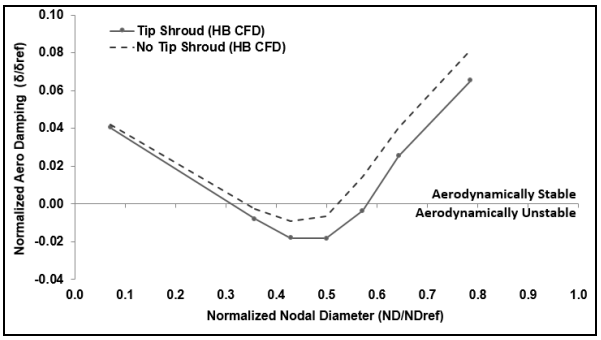

Figure 10: Comparison of shrouded (axisymmetric) and unshrouded aerodynamic damping predictions

A similar trend in which the maximum relative errors were observed at the min and max damping locations was encountered for a similar study performed on the blade with the axisymmetric tip shroud previously shown in Figure 7. The range of nodal diameters which correspond to the lowest point of stability are shown in Figure 10. In this case, both the shrouded and unshrouded solutions were obtained using the HB Flutter solver at equivalent operating conditions. The maximum relative errors for the axisymmetric simulation again corresponded to the location of minimum stability, which is represented by the normalized nodal diameter range of [0.4, 0.6] of Figure 10.

What is different in this case however is that the unshrouded simulation over-predicted the aerodynamic damping at the location of maximum error, whereas the opposite was true for the previous blade shown in Figure 9. This difference exists because both blades undergo relative motions that are unique to their own aerodynamic and structural responses. Specifically, variations in blade count, shroud contact, stiffness etc… all contribute in influencing the mode shape and vibration frequency of the blade. Therefore the way in which the motion interacts with the resolved pressure field could in fact yield a difference in loading that may either dampen or excite the prescribed motion. This goes to show that neglecting the tip shroud from the aerodynamic simulation does not consistently produce a more or less conservative estimate for the aeroelastic response. It does however consistently demonstrate an error in the solved damping coefficients at the minimum and maximum points of stability. This margin of error should be taken into consideration especially if the predicted minimum damping values fall close to the critical flutter boundary.

FLUTTER VALIDATION LIMITATIONS

Turbomachinery flutter is a particularly difficult phenomenon to test under real operating conditions. Measurements of unsteady pressure in simple rig tests with imposed airfoil motion have typically been used to validate computational models for pressure prediction. However, a viable method for validating the damping characteristics of an actual shrouded turbine blade in its true operating environment remains elusive.

Strain gauge data has been used in the past by Scalzo et al. (1986) to evaluate the “effects” of flutter in terms of induced strain due to blade displacement during vibrating motion. Tip timing methods such as mentioned in Torkaman et al. (2017) have also been used to directly measure relative blade displacement, but displacement is a function of other variables including mechanical properties in addition to the coupled aerodynamic contribution resulting from unsteady pressure. For example if mechanical damping is large enough, it may still dampen the excitation caused by

the aerodynamic contribution and prevent flutter (Rice et al. 2009). Therefore to accurately correlate computational models to an actual event, the sum of all non-aerodynamic damping must be known and compared to the aerodynamic contribution to assess the total stability of the system.

Non-aerodynamic damping is generally attributed to a viscous portion associated with internal material damping, and a non-viscous portion associated with dry friction due to rubbing motion of adjacent hardware such as the blade root, under-platform dampers, and shroud tips. In the case of shrouded blades, a significant portion of non-aerodynamic damping is due to the rubbing motion between adjacent shrouds. Due to the nonlinearity of frictional forces however, the non-viscous damping is highly nonlinear and very difficult to assess.

For these reasons, the determination of when exactly aerodynamic damping becomes negative (as a function of some parameter such as engine load or stage mass flow) cannot currently be accomplished in a rig test. In fact, the only known method to truly validate the flutter margin of a shrouded turbine blade remains an actual engine test. Such tests however, are designed mainly to clear the operating envelope of the engine from flutter rather than explore its onset as an actual event would be truly catastrophic.

CONCLUSIONS

A method to incorporate complex interlocked tip shroud geometry into aerodynamic flutter simulations has been presented. Differences in the predicted steady and unsteady pressure fields of a shrouded industrial gas turbine blade were observed between 60-100% span when compared to an equivalent simulation that neglected the presence of the tip shroud. The variations in the pressure fields were found to influence the aerodynamic damping predictions at the minimum and maximum points of stability for the 1st Torsional modes of two separate shrouded blades. The simulations exhibited similar trends in terms of relative error near the minimum and maximum aerodynamic damping locations, however under- or over-prediction behavior of the aerodynamic damping was not consistent due to known differences in geometrical and structural properties between the two blades.

The proposed tip shroud treatment introduces a higher level of aerodynamic fidelity into the flutter prediction as the corresponding fluid flow-structure near the tip region is more-representative of the blade's true operating environment. Although it may sometimes be more practical to neglect the tip shroud geometry from the numerical simulation, the resulting over-tip flow interaction may introduce an error into the aerodynamic damping prediction of the blade. The uncertainty may be problematic for cases where the predicted aerodynamic damping falls short of the flutter boundary and the associated (unknown) margin of error lies beyond the unstable threshold. The proposed method mitigates this uncertainty by permitting the aeroelastic calculation to incorporate a better representation of the aerodynamic flow structure near the tip region of the shrouded blade.

REFERENCES

Carta, F.O., (1967), *Coupled Blade-Disk-Shroud Flutter Instabilities in Turbojet Engine Rotors*, Journal of Engineering for Gas Turbines and Power, Vol. 89 p. 419-426.

Collar, A.R., (1946), *The Expanding Domain of Aeroelasticity*, Journal of the Royal Aeronautic Society, Vol. 50, p. 613-636, August.

Custer C.H, Weiss J.M, Subramanian V, Clark W.S, Hall KC., (2012), *Unsteady Simulation of a 1.5 Stage Turbine Using an Implicitly Coupled Nonlinear Harmonic Balance Method*, ASME. Paper No. GT2012-69690.

Gnesin, V., Kolodyazhnaya, L., Rzadkowski, R., (2000), *Coupled Aeroelastic Oscillations of a Turbine Blade row in 3D Transonic Flow*, Journal of Thermal Science, Vol. 10, No. 4 p. 318-324.

Hall H.C., Thomas J.P., Clark W.S.,(2002), *Computation of Unsteady Nonlinear Flows in Cascades Using a Harmonic Balance Technique,* AIAA Journal Vol 40, No.5 May p 879-886.

Kielb R., Barter J., Chernysheva O., Fransson T., (2006), *Flutter Design of Low Pressure Turbine Blades with Cyclic Symmetric Modes*. In: Hall K.C., Kielb R.E., Thomas J.P. (eds) Unsteady Aerodynamics, Aeroacoustics and Aeroelasticity of Turbomachines. Springer, Dordrecht, p 41-52.

Marshall, J.G., Imregun, M., (1996), *A Review or Aeroelasticity Methods with Emphasis on Turbomachinery Applications*, Journal of Fluids and Structures, V. 10 p. 237-267.

Marshall J.G., Giles M.B., (1998), *Some Applications of a Time Linearized Euler Method to Flutter & Forced Response in Turbomachinary*, T.H. Fransson, Unsteady Aerodynamics and Aeroelasticity of Turbomachines; p 225-240.

McBean I., Hourigan K., Thompson M., Liu F., (2005), *Prediction of Flutter of Turbine Blades in a Transonic Annular Cascade*, Journal of Fluids Engineering, Vol. 127 p. 1053-1058.

Ning W., He L., (1998), *Computation of Unsteady Flows Around Oscillating Blades Using Linear and Nonlinear Harmonic Euler Method*, Transactions of ASME, Vol 120 July p508-514.

Pinelli L., Poli F., Arnone A., Schipani C., (2009), *A Time-Accurate 3D Method for Turbomachinery Blade Flutter Analysis*, 12th International Symposium on Unsteady Aerodynamics, Aeroacoustics and Aeroelasticity of Turbomachines (ISUAAAT). September 1–4, 2009, London, UK. Paper I12-S8-3.

Rice T., Bell D., Singh G., (2009), *Identification of the Stability Margin Between Safe Operation and the Onset of Blade Flutter*, Journal of Turbomachinery, Vol. 131, p. 011009-1-10.

Scalzo A.J., Allen J.M., Antos R.J., (1986), *Analysis and Solution of a Nonsynchronous Vibration Problem in the Last Row Turbine Blade of a Large Industrial Combustion Turbine*, Journal of Engineering for Gas Turbines and Power, Vol. 108/591.

Siemens PLM Software, (2018), *Simcenter STAR-CCM+ User Guide*, STAR-CCM+ version 13.04.011-R8.

Teixeira, M. A., Kielb, R. E.,(2017), *Tip Clearance Influence on Aerodynamic Damping Maps*, Proceedings of 12th European Conference on Turbomachinery, April 3-7 2017, Stockholm, Sweden, Paper ID: ECT2017-300.

Torkaman, A., Vogel, G., Fiebiger, S., Dietrich, D., Washburn, R., (2017), *Gas Turbine Cycle Upgrade and Validation for Heavy Duty Industrial Machines*, ASME Paper No. GT2017-64173.

Waite, Kielb, (2015), *The Impact of Blade Loading and Unsteady Pressure Bifurcations on Low-Pressure Turbine Flutter Boundaries*, ASME Paper No. GT2015-42857.

Weiss J.M, Subramanian V, Hall K.C., (2011), *Simulation of Unsteady Turbomachinery Flows Using an Implicitly Coupled Nonlinear Harmonic Balance Method*, ASME Paper No. GT2011-46367.